Micrometeoroid flux in the inner Solar System

The major sources of the dust population in the inner Solar System are asteroid collisions and debris released from short period comets. The products of cratering and fragmentation events in the asteroid belt are at the origin of dust bands observed in IRAS data (Low et al. 1984, Hauser et al. 1984). These bands were interpreted as dust deriving from the continuous collisional activity in the asteroid furnishing a constant supply of debris (Dermott et al. 1984, Sykes and Greenberg 1986). The dust grains produced in the asteroid belt slowly evolve under solar radiation forces and the gravitational force of the Sun and planets. In particular, particles smaller than 1 *cm* are significantly perturbed by Poynting-Robertson and solar wind drag and spiral towards the Sun with timescales that depend on their size and composition (Burns et al. 1979).
During their journey they may not only be gravitationally scattered by terrestrial planets but also be trapped into one or more mean motion resonances (Jackson and Zook 1992, Marzari and Vanzani 1994, Marzari et al. 1996). Due to the interplay between the gravitational perturbations of the planets and the Poynting-Robertson drag, the orbital evolution can be quite complex. As a consequence, models based on a uniform and steady flux of dust grains from the Main Belt into the inner regions of the Solar System may not be appropriate. A full numerical approach is needed to estimate how the grain population evolve while approaching the Sun. Meteoroid impacts have a very important role in the evolution of planets and satellites like Mercury and Moon having a direct effect on their surface and exosphere. Since the exobase is presently on the surface of the planet or satellite, the sources and sinks of the exosphere are tightly linked to the composition and structure of the planet surface.
Different mechanisms and source processes have been proposed as possible sources of elements like sodium and potassium in the exosphere of Mercury and Moon (Hunten and Sprague 1997; Killen and IP 1999), including sputtering by the solar wind, photon-stimulated desorption (Madey et al. 1998; Mendillo et al. 1999; Yakshinskiy and Madey 2004), thermal desorption (Yakshinskiy and Madey 2000), and micrometeoroid impacts (Cintala 1992; Mendillo and Baumgardner 1995; Cremonese and Verani 1997; Verani et al. 1998; Smith et al. 1999). But a significant fraction of volatiles released into the exosphere of Mercury is thought to be produced by impact vaporization of meteoritic material on the surface (Cremonese et al. 2005).
When dust particles enter the planet's atmosphere at orbital speeds, they decelerate and go through a process named ablation. In fact, meteoroids penetrating the atmosphere are accelerated by the planetary gravitational field and slowed down by collisions with atmospheric elements that remove part of the mass and heat the particle surface producing an additional loss of mass by evaporation. The interaction of high-speed meteoroids and atmospheric gases can lead to the deposition in the planetary atmosphere of species that would otherwise be absent such as Fe and Mg. So meteoritic influx therefore modifies vertical profiles of plasma density in a planetary ionosphere (Molina-Cuberos et al. 2008, Withers 2008). On entering the Earth's atmosphere, most particles in the micrometer size range are melted during atmospheric deceleration. Because of its low surface gravity and his atmosphere considerably thinner than that of Earth, Mars is a favorable planet for the study of unaltered rest of micro-meteoritic dust grains after the atmospheric entry.

We may distinguish two populations of meteoroids depending on their dynamical evolution: small particles ($r < 1$ *cm*) dominated by the Poynting-Robertson drag, and large particles ($r > 1$ *cm*) driven by gravity only.
We study the long-term evolution of dust grains (i.e., $r < 100$ μm) from main-belt asteroids (hereafter MBA) and Jupiter-family comets (hereafter JFC) to planets in the inner solar system and the Moon using a dynamical evolution model that follows the orbital path of particles under the effects of the gravitational and non-gravitational forces. By means of numerical simulations, we estimate the flux of dust particles and their impact velocity distribution.

We use the dynamical evolution model of dust particles of Marzari and Vanzani (Marzari and Vanzani 1994). It numerically integrates a (N+1)+M body problem (Sun + N planets + M body with negligible mass) with the high-precision integrator RA15 (Everhart, 1985). Radiation and solar wind pressure and Poynting-Robertson drag are included as perturbative forces together with the gravitational attractions of all the planets in the Solar System.

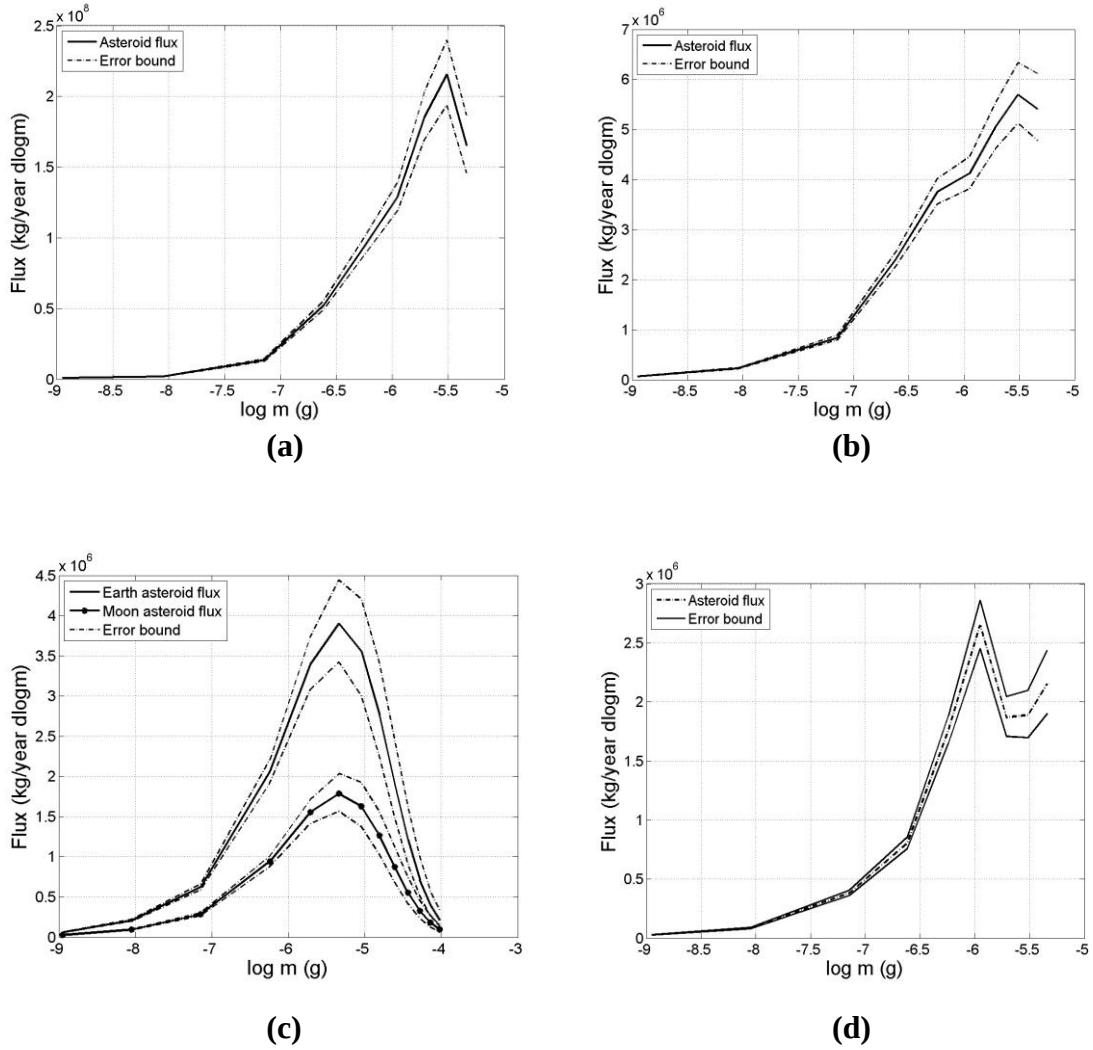

Fig. 1. Micrometeoritic flux on a) Mercury; b) Venus; c) Earth and Moon; d) Mars.

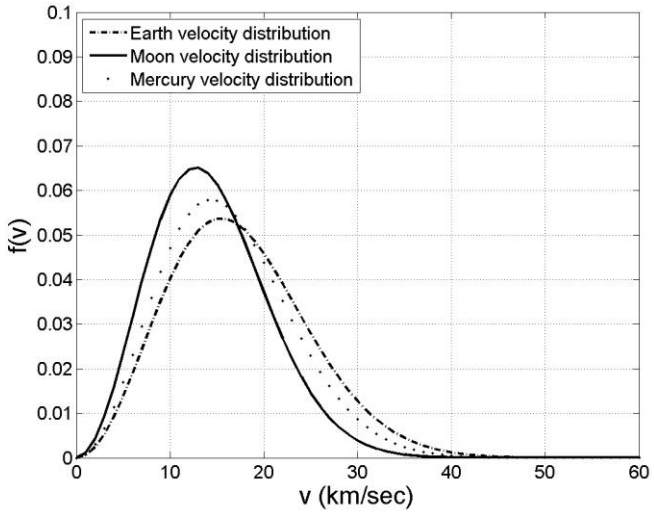

Fig. 2. Comparison of velocity distribution curves on Mercury, Earth and Moon.

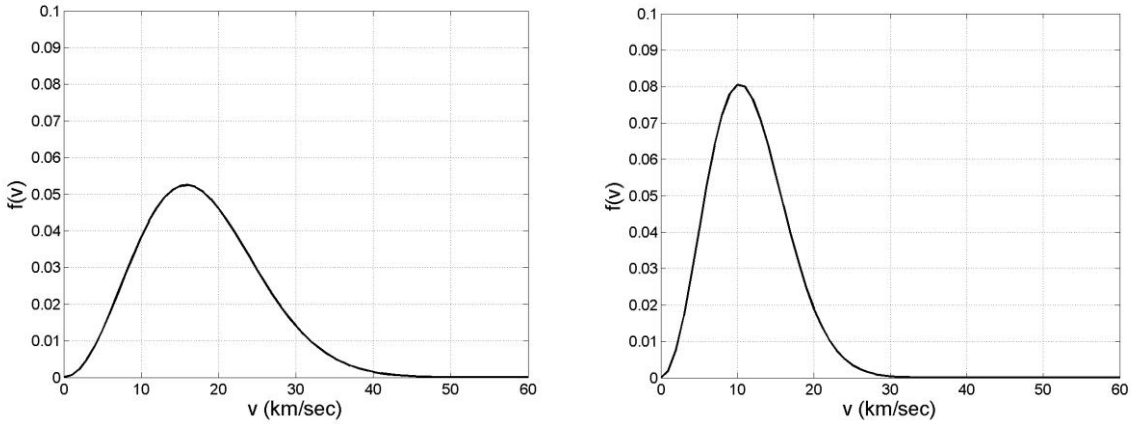

(a) **(b)**

Fig. 3. Velocity distribution curves on a) Venus; b) Mars.

	Comets				**Asteroids**			
Particle size (μm)	**Mercury**	**Venus**	**Earth**	**Mars**	**Mercury**	**Venus**	**Earth**	**Mars**
10	25.8	19.9	28.7	25.6	37.6	27.7	24.8	9.8
50	19.0	17.3	29.5	34.2	32.1	26.5	22.9	18.5
100	12.9	15.9	27.1	44.0	30.7	30.9	23.2	15.2

Table 1. Percentage of particle arriving on Mercury, Venus, Earth and Mars considering cometary and asteroidal sources

Planetary body	Asteroidal mean velocity (km/sec)	Cometary mean velocity (km/sec)
Mercury	16.81	17.59
Venus	14.19	20.85
Earth	18.60	16.87
Moon	15.04	12.84
Mars	9.10	13.57

Table 2. Velocity values of asteroidal and cometary dust at different planets and Moon.

Table 2 shows the mean velocity values of asteroidal and cometary impacting particles. A substantial difference in the mean velocity values of asteroidal and cometary dust particles can be observed for all planets. This may be ascribed to the initially different distribution and to the different dynamical paths. In particular, while for small particles the Poynting-Robertson drag is dominant, resonant effects and close approaches have a central role for larger particles and introduce effects that cannot be simply scaled out with radial distance. For Mars the dust particles coming from the main belt are not strongly affected by dynamical effects, so that their distribution resembles the original distribution and the impact velocity is low. However, as soon as the particles reach Earth, the impact speed increases because of the different dynamical mechanisms that excite the eccentricity in particular. At Venus the impact speed is lower, possibly because of progressive circularization through Poynting-Robertson drag, and finally, at Mercury it is high again because of the fast Keplerian period and the possibility of impacts of particles with high eccentricity at perihelion. The mean impact velocities of cometary particles are instead significantly higher for Mars and Venus, while they are comparable for the other bodies. For Mars, the reason is that the grains did not have enough time to be circularized during their drift so that their inclinations and eccentricities are higher than the dust of asteroidal origin. For Venus, close encounters with Earth lead to a new peak in eccentricity when they encounter the planet, in most cases close to perihelion, even higher than that at Mars. This leads to the high impact speeds in particular for larger grains, which are damped by PR-drag on a longer timescale. The two different dust sources have typical impact speeds that are also different at Earth, but in this case, the reverse occurs: the mean velocity value of asteroidal dust particles is higher than the cometary velocity. This might be an effect of the frequent resonant trapping around the planet during which the eccentricity is slowly pumped up. Resonances rarely occur for cometary grains.

Planetary body	Estimeted dust flux (kg/y)	Flux ratio planetary body/Earth
Mercury	$(1.97\pm0.17)\cdot 10^{8}$	35.14
Venus	$(6.91\pm0.55)\cdot 10^{6}$	1.23
Earth	$(5.60\pm0.96)\cdot 10^{6}$	1
Moon	$(3.66\pm0.44)\cdot 10^{6}$	0.65
Mars	$(2.96\pm0.23)\cdot 10^{6}$	0.53

Table 3. Estimated flux values at different planets and Moon.

A natural consequence of the estimate of the flux is the computation of the vapor and neutral atoms production rates on Mercury and Moon, as due to the impacts of micrometeoroids. We consider the size range between 5-100 μ*m*. According to Bruno et al. 2007 and Cremonese et al. 2005 the production of neutral Na atoms on Mercury and Moon is mainly due to meteoroids larger than 10^{-5} *m*. As a consequence, approximately 50% of the Na comes from impacting meteoroids in the size range $5*10^{-6}$ -10^{-4} *m*, 43% from 10^{-4}-10^{-3} *m*, 6% from 10^{-3} -10^{-2} *m* and the remaining 1% from meteoroids with size larger than 1 cm.

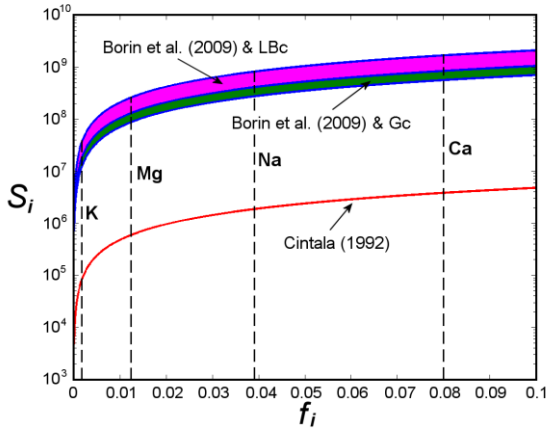

Fig. 3. Production rate f_i (*Number of atoms cm^{-2} s^{-1}*) with different weight percentages of atoms on the surface of Mercury.

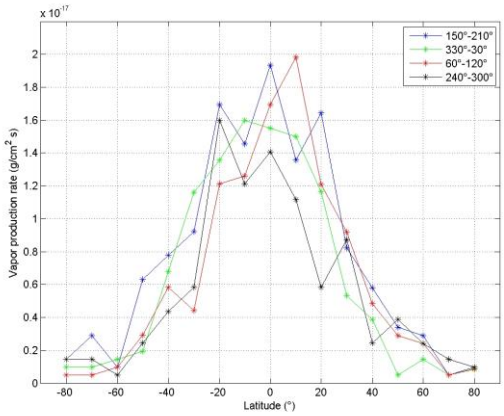

Fig. 4. Vapor production rate due to micrometeoroid flux on the Moon in four different sectors of the lunar orbit (the apogee 330−30◦, the perigee 150−210◦, 60◦−120◦, and 240◦−300◦) as a function of the latitude.

Figure 4 reports the results of our model on micrometeoroid flux impacting the Moon and the number of sodium atoms released. We obtained the number of Na atoms as 1.648 Å~ 10^5 atoms/cm^2 s, which is higher than the value of other authors, suggesting that the impact process due to micrometeoroids can play a very important role in the contribution of neutral atoms to the exosphere. Previous estimates assumed that the micrometeoroid impacts are a negligible source, about 1%, compared to the value of 2 Å~ 10^6 atoms/cm^2 s produced by PSD (Morgan et al. 1989; Sarantos et al. 2010). Our new evaluation of the impact vaporization mechanism raises the contribution to the 8% of PSD at the subsolar point. Assuming that the PSD rate decreases as the cosine of the solar zenith angle, while our dynamical model shows no asymmetry in longitude for the micrometeoroids flux, the contribution of the impact vaporization becomes similar nearby the dawn and dusk regions and dominant in the night side.
Our result shows that impact vaporization is also very similar to the ion sputtering mechanism at the subsolar point, that is 2.65 Å~ 10^4 atoms/cm^2 s (Sarantos et al. 2010), and is dominant for other longitudes.

References.

[1] Borin, P et al. 2017, Dust flux in the inner solar system, A&A, 605

[2] Bruno, M. et al. 2006, Neutral sodium atoms release from the surface of the Moon induced by meteoroid impacts, Mon. Not. R. Astron. Soc., 367, pp. 1067-1071

[3] Burns, J. A. et al. 1979, Radiation Forces on Small Particles in the Solar System, Icarus 40, pp. 1-48

[4] Cintala, M. J. 1992, in Journal of Geophysical Research Volume 97, Impacted-Induced Thermal Effects in the Lunar and Mercurian Regoliths

[5] Cremonese, G., & Verani, S. 1997, High resolution observations of the sodium emission from the moon, Adv. Space Res., 19, 1561

[6] Cremonese, G. et al. 2005, Release of neutral sodium atoms from the surface of Mercury induced by meteoroid impacts, Icarus, 177, pp. 122-128

[7] Cremonese, G., P. Borin, E. Martellato, F. Marzari, M. Bruno: *New Calibration of the Micrometeoroid Flux on Earth*, Astrophys. J. Lett. 749, L40,1–4, 2012a.

[8] Dermott, S. F. et al. 1984, Origin of the solar system dust bands discovered by IRAS, Nature, vol. 312, pp. 505-509

[9] Everhart, E. 1985, Dynamics of Comets: Their Origin and Evolution, Proc. IAU Coll. 83, p. 185

[10] Hauser, M. G. et al. 1984, IRAS observations of the di_use infrared background, Astrophysical Journal, Part 2, vol. 278, pp. L15-L18

[11] Hunten, D. M., & Sprague, A. L. 1997, Origin and character of the lunar and Mercurian atmospheres Adv. Space Res., 19, 1551

[12] Killen, R. M., & Ip, W-H. 1999, The surface-bounded atmospheres of Mercury and the Moon, Rev. Geophys., 37, 361

[13] Jackson, A. A. and Zook, H. A. 1992, Orbital evolution of dust particles from comets and asteroids, Icarus, vol. 97, pp. 70-84

[14] Love, S. G. and Brownlee, D. E. 1993, A Direct Measurement of the Terrestrial Mass Accreation Rate of Cosmic Dust, Science, Vol. 262

[15] Low, F. J. et al. 1984, Infrared cirrus - New components of the extended infrared emission, Astrophysical Journal, Part 2, vol. 278, pp. L19-L22

[16] Madey, T. E., Yakshinskiy, B. V., Ageev, V. N., et al. 1998, Desorption of alkali atoms and ions from oxide surfaces - Relevance to origins of NA and K in atmospheres of Mercury and the moon, J. Geophys. Res., 103, 5873

[17] Mendillo, M., & Baumgardner, J. 1995, Constraints on the origin of the Moon's atmosphere from observations during a lunar eclipse, Nature, 377, 404

[18] Mendillo, M., Baumgardner, J., Wilson, J., et al. 1999, Observational Test for the Solar Wind Sputtering Origin of the Moon's Extended Sodium Atmosphere , Icarus, 137, 13

[19] Marzari, F. and Vanzani, V. 1994, Dynamical Evolution of Interplanetary Dust Particles, Astronomy and Astrophysics 283, 275-286.

[20] Marzari, F. et al. 1996, Collision Rates and Impact Velocities in the Trojan Asteroid Swarms, Icarus 119, 192-201

[21] Molina-Cuberos, J. G. et al. 2008, Meteoritic Layers in Planetary Atmospheres, Space Sci Rev, 137, pp. 175191

[22] Sykes, M. V. and Greenberg, R. 1986, The formation and origin of the IRAS zodiacal dust bands as a consequence of single collisions between asteroids, Icarus, vol. 65, pp. 51-69

[23] Yakshinskiy, B. V., & Madey, T. E. 2000, Desorption induced by electronic transitions of Na from SiO_2: relevance to tenuous planetary atmospheres. Surf. Sci., 451, 160

[24] Yakshinskiy, B. V., & Madey, T. E. 2004, Photon-stimulated desorption of Na from a lunar sample: temperature-dependent effects Icarus, 168, 53

[25] Withers, P. et al., 2008, Physical characteristics and occurrence rates of meteoric plasma layers detected in the Martian ionosphere by the Mars Global Surveyor Radio Science Experiment, Journal of 0eophysical Research, Vol. 113